



An evolutionary shape optimization for elastic contact problems subject to multiple load cases

Wei Li ^a, Qing Li ^{b,*}, Grant P. Steven ^c, Y.M. Xie ^d

^a School of Aerospace, Mechanical and Mechatronic Engineering, The University of Sydney, NSW 2006, Australia

^b School of Engineering, James Cook University, Townsville, QLD 4811, Australia

^c School of Engineering, University of Durham, Durham DH1, 3LE, United Kingdom

^d School of Civil and Chemical Engineering, Royal Melbourne Institute of Technology, GPO Box 2476V, Melbourne, VIC 3001, Australia

Received 20 January 2004; received in revised form 23 August 2004; accepted 6 December 2004

Abstract

Most structures in the real life are subject to multiple load cases. This paper aims at extending the evolutionary structural optimization (ESO) algorithm to optimal contact shape design for elastic bodies under the multiple load cases. To evaluate the reference stresses of each contact node in a finite element framework, an extreme stress criterion (the worst case design) and a weighted average criterion (Pareto design) are presented. In the extreme stress method, the highest nodal contact stress under all load cases is adopted as the reference level. In the weighted average method, the weighted sum of nodal contact stresses over all the load cases is regarded as the reference. It is found that these two criteria can produce different results. In this paper, the examples are presented to demonstrate some new features of contact shape optimization in the presence of the multiple load cases.

© 2005 Elsevier B.V. All rights reserved.

Keywords: Finite element analysis; Unilateral constraint; Elastic contact; Multiple load cases; Shape optimization

1. Introduction

Designers are often faced with the problem of optimization of a structure that is subjected to multiple load cases. The term “multiple load case” here means groups of loads that act independently at different times in the structural lifecycle. In the course of its life, a structure is usually required to sustain several

* Corresponding author. Tel.: +61 7 4781 5762; fax: +61 7 4781 4660.
E-mail address: qing.li@jcu.edu.au (Q. Li).

different types of load sets, each of which can induce a totally different type of structural response. Frequently, these loading conditions are completely independent of each other in the sense that they scarcely act upon the structure at the same time. As a consequence of this, it is usually hard even for the most experienced designer to identify the most critical load case for the design. It is highly desirable that the design would be suitable for all the load cases under the prescribed criteria. Unfortunately, this is often extremely difficult if not impossible. In a certain sense, the design in a multiple load environment can be to pursue an optimum compromise.

Structural shape optimization problems involving multiple loading conditions can be broadly divided into two categories. One type concerns the optimization of stiffness, natural frequencies and other objective functions relative to each individual loading condition. This forms a multiple objective optimization problem [1]. The other type involves finding the optimal shape for one of the most critical objectives, at the same time satisfies certain constraints, such as allowable displacements, stresses and natural frequencies in relation to all loading conditions. This presents a single objective optimization problem involving multiple constraints [2]. As pointed out by Adali [3], the main difference between a multi-objective design and a constrained design is that the former behaves more interactively and could provide a family of designs to explore the best possible alternatives.

There are a limited number of reports in the literature concerning structural optimization involving multiple loading conditions, which is the situation that designers actually encounter in creating structural designs. Botkin developed a two-dimensional shape optimization approach with adaptive mesh refinement over multiple loading conditions [4]. Diaz and Bendsøe extended the well-established Homogenization algorithm to multiple load cases, where the objective function was constructed in terms of the weighted average of all mean compliances [5]. Following this technique, Bendsøe et al. further demonstrated a number of optimization problems for continuum structures subjected to the multiple loading conditions [6,7]. Shimoda et al. also introduced a differentiable Kreisselmeier–Steinhauser global integral function to scalarize the multi-objectives of the mean compliances corresponding to individual loading [8]. Gutkowski and Dems presented an optimality criteria algorithm based on the Kuhn–Tucker theorem in two-dimensional shape optimization, in which the multiple loading conditions were represented in the problem of equality conditions of a set equilibrium equations for each loading case separately [9]. Haridas and Rule used a modified interior penalty algorithm to treat all the load cases simultaneously, where the multiple load case problem was transformed into an equivalent single load case by means of a pseudo-constraint vector [10]. O'Brien and Dixon described the use of algebraic linear programming for optimal design of pitched roof frames subject to multiple load conditions [11]. Papadrakakis et al. thoroughly considered an Evolutionary Algorithm (EA) for both static and seismic load conditions in large-scale design problems, where a number of accelerograms were produced from the elastic design response spectrum of the region and then was used to constitute the multiple loading conditions for optimal designs [1,12]. In favor of the well-known fully stressed design, Mueller et al. exhaustively investigated the relation of structural responses under multiple load cases with the Pareto frontier [13]. To formulate a combined sensitivity for the multiple load cases, the weighting coefficients were determined in terms of the ratios of structural responses to the corresponding constraints in the work by Chu et al. [2] and Wang et al. [14], where the method was shown in consistency with the Kuhn–Tucker condition.

Different from the approaches to the equal or compromised consideration of all load conditions as mentioned above, Xie and Steven took into account the highest elemental stress level (*the worst case*) over all load cases for identifying the extreme efficiency of material usage [15,16]. Those elements with the least efficiency under all load conditions are progressively removed until the remaining elements become relatively efficient for at least one of all the load cases. As an extension to Xie and Steven's work, Young et al. reported a bi-directional evolutionary topology optimization approach to both two- and three-dimensional structures subjected to the multiple load cases [17]. Here again, elements are removed only if they are inefficient for all the load cases, but added if needed for just one load case.

It is found that the existing literature mainly involves some linear structural systems. In other words, whatever the complexity of load conditions, the structural stiffness matrix remains unchanged. As a result of this, the cost of finite element analysis for the multiple load cases would be nearly the same order as that for a single load case. More importantly, in spite of the different load conditions, the structural responses are linearly characterized, in which the principle of superposition can be always applied. To a certain extent, this appears relatively simple for design optimization and may not increase the difficulty of the design trade-off too much [18,19].

In elastic contact systems, multiple load cases are very common. For example, surface contact stress of a bearing depends on the magnitude and direction of the applied loads. For a washer of fastener system the contact stress relies on the initial torque produced from the spanner. In these examples, the load cases can be applied at the different locations (e.g. bearing) or the same location but in different magnitudes (or directions) and at different times (e.g. washer).

Due to the high non-linearity of unilateral contact systems, the incremental stiffness matrices (i.e. a tangential stiffness matrix based on a linearization of governing equilibrium equation) need to be decomposed individually for each load case. This implies that the structural responses of elastic contact systems may be of a higher order of difference than those of linear elastic systems. Consequently, there would appear greater difficulty to achieve a best possible compromise for all load cases. In a review article, Esping described a practical example of contact shape optimization subjected to multiple load cases [20]. The contact stress peak was remarkably reduced through the shape optimization of contact components. Late, Kocvara et al. formulated an optimal problem of unilateral contacts subjected to multiple load cases, where the minimum of the potential energies over the load cases is considered as the objectives [21]. They recognized that only a “better” design could be achieved for this type of problem, which to a certain extent depends upon the designer’s preference and design criteria adopted. A conservative way that they suggested was to look for the so-called the *worst case design*. In a later version of their study [22], they mathematically proved the existence of a solution to the continuum elasticity under multiload cases, where the total potential energies were minimized in a sense of the worst case. In effect, the minimization problem of potential energies presents no significant difference in the algorithms with those of traditional stiffness maximization problem but introducing multiple unilateral contact conditions [21]. To the authors’ best knowledge there has been inadequate report, to date, regarding the contact shape optimization subjected to multiple load cases in spite of its great significance. Moreover, there was a fundamental lack of a thorough analysis and comparison in the multiple solutions. A further endeavor to explore such a problem would be considerably beneficial from both a theoretical and a practical perspective.

This paper aims at extending the well-established ESO algorithm to the optimum shape designs of elastic contact problems under the multiple load cases. Unlike the single load case [23–25], there will be the same number of contact stress levels as the load case number for each contact pair. One of the major problems associated with this type of structural system is to determine the reference stress level for each contact pair. In this study, two practical criteria, namely the *extreme stress criterion* (the worst case design) and the *weighted average criterion* (Pareto design), are presented. The highest nodal contact stress over all load cases is taken into account in the former, while the weighted average stress under all load cases is regarded as the design reference in the latter. It is found that these two design criteria may lead to different optimal shapes.

2. Finite element modeling of contact problem

The contact of one body with another is an aspect of the mechanics of solids that is mathematically very challenging. The underlying difficulty is that contact problems are highly nonlinear: the contact area may not be known prior to the application of loads, the contact state and area may change during the loading process, and complex physical phenomena present on the contact surfaces often require special mechanical

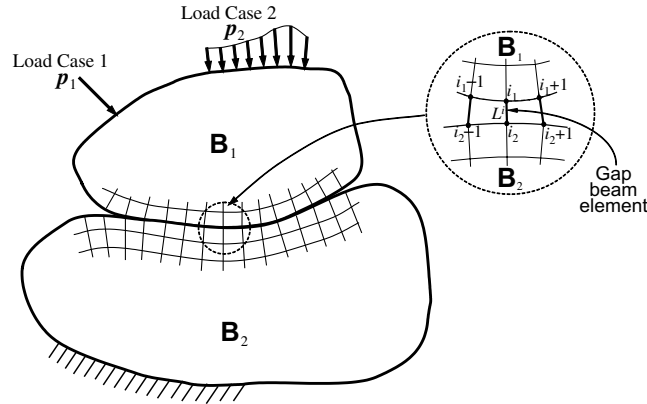


Fig. 1. Finite element modeling for contact problem.

and mathematical considerations [26]. In the last three decades, significant advances have been made in the numerical solution of the unilateral contact problems using finite element techniques [27].

Fig. 1 illustrates the finite element modeling of two elastic bodies B_1 and B_2 in a possible contact state. Without loss of generality, it is assumed that body B_2 has a kinematical boundary condition while body B_1 is acted upon by two load cases p_1 and p_2 . Let the pairs of boundary nodes i_1 and i_2 ($i = 1, 2, \dots, M$) be the points where contact may occur at some stage of the contact process. Once these corresponding contact nodes are defined on both the contact surfaces and their contact states are classified, contact stresses can be obtained by a non-linear finite element analysis.

To emulate the contact state, which changes during the loading process, a simple approach is to introduce *compression-only gap beam elements*, which have been adopted by many finite element structural analysis packages, e.g. G + D Strand6 [28]. These gap elements are designed to resist compression only and are automatically removed from the analysis if placed in tension.

In the process of finite element analysis, the two contact bodies are modeled individually and the contact surfaces are separated by a very small gap. As indicated in Fig. 1, the contact node pairs are joined together by gap elements connected across the initial spacing between these two contact surfaces. At the initial condition, all the gap elements are neither in compression nor in tension. The initial gap length indicates a critical contact state. Any consequence of loading that makes the spacing smaller would put the gap elements in compression and the beams need to possess an artificially high axial stiffness to transfer the forces between the two bodies and to prevent one body from penetrating into another. Alternatively, any consequence of loading that makes the spacing larger would put the gap elements in tension and cause it to be automatically removed from the analysis.

With such a special treatment in contact, these two contact bodies are considered as a whole. As a result, the equilibrium equation of the entire system can be expressed in a linearized finite element form as

$$K_j u_j = p_j \quad (j = 1, 2, \dots, N) \tag{1}$$

where p_j denotes the loading vector of the j th load case and K_j the corresponding global tangential stiffness matrix of the structural system. Unlike the linear elastic system with single deformable body, the justification of contact status can hardly be achieved in one step. In general, a step-by-step incremental method is required in a fashion of Newton-Raphson iterations as in [29].

In this study, G + D Strand6 solver [28] was employed for the contact finite element analysis. To implement the gap beam elements, a regular matching node-to-node mesh across the contact interface is required, as illustrated in Fig. 1. When necessary, different element types may be applied as far as

the interfacial nodes can be matched. For elastic contact problems, it is also assumed that a small contact deformation (either sticking or slipping with or without friction) is taken place in a conforming form over the mesh. In the FE solver, a rigorous contact search algorithm is applied for each linear iteration.

Although G + D Strand6 finite element solver is employed as an analysis tool in this study, the proposed ESO contact algorithm can be directly accommodated to other finite element formulations. Furthermore, ESO itself does not require the node-to-node mating mesh [23,24], which allows a substantial sliding over the interface and the freedom of meshing. In practice, human and animal biting motion is one of such examples, where slipping between upper and lower teeth can be very significant and the contact modeling and analysis become more complex. It is worth pointing out that the investigation of contact algorithms is beyond the scope of this paper. The existing finite element methods are taken only as an analysis engine for the design optimization.

3. Design criteria for multiple load cases

In a multiple load case system, a designer has to take all extreme design load conditions into account in order to most possibly cover different structural situations in the design. From these multiple solutions to the structural system, one needs to determine which load conditions are of crucial importance in the structural behavior. This implies that a design could depend heavily on the judgment and skill of the designer. In this sense, the design appears more like an art than a science. In other words, different people may have different views and objectives that may lead to totally different designs. In practice, it is hard to make a unified criterion that suits all design requirements and strategies.

More difficultly, some load cases and the corresponding design criteria may be in discord with one another in what they are set out to achieve. Such a dilemma in conflicting objectives exists in numerous practical contact systems. This further increases the complexity of solving contact shape optimization subjected to the multiple load cases.

There are mainly two types of objective functions $f(g(\mathbf{x}))$ reflecting the unilateral contact optimization subjected to single load case in literature [30]. Note that in the optimal problem, the design variable can usually be the gap function $g(\mathbf{x})$ between potential contact node pairs on the contact bodies [31,32]. The first class of optimality criterion, more inherent in engineering applications, is to minimize the maximum contact stress or to achieve a uniform contact stress distributions over the contact profile, which may be mathematically stated as [23,24,33]

$$f(g(\mathbf{x})) = \max_i [\sigma^i(g(\mathbf{x}))] \quad (2)$$

where i indicates the i th contact pair ($i = 1, 2, \dots, M$). In spite of their practical significance, unfortunately, the non-differentiability of such an objective function, to a certain extent, prevents the widespread application of mathematical programming techniques.

The second class of optimality criterion, and less intuitive, is to minimize the potential energy $U(g(\mathbf{x}))$ attained in equilibrium,

$$f(g(\mathbf{x})) = U(g(\mathbf{x})) = \frac{1}{2} \boldsymbol{\sigma}^T \mathbf{C} \boldsymbol{\sigma} \quad (3)$$

where \mathbf{C} denotes the flexibility matrix of the contact surface [34]. Eq. (3) gives an estimation of strain energy stored in the body due to contact tractions. This usually leads to some convenient mathematical and computational features (such as being differentiable) in addition to resulting in a uniform contact stress distribution. On this aspect, Haslinger, Klarbring and their co-workers have devoted great efforts in relation to the mathematical groundwork since 1980s [31]. The major work has been collected in the Ref. [32].

The evolutionary approach developed in this paper characterizes heuristic, in which the gradient information is not required. Hence, the first class of objective function, as in Eq. (2), namely the min-max or the uniformity of contact stress, is adopted because of its direct relevance to practical issues such as wear and fretting.

Consider N different load cases \mathbf{p}_j ($j = 1, 2, \dots, N$) applied to the contact system. Each may yield a completely different contact stress distribution $\sigma(\mathbf{p}_j, \mathbf{g})$. For dealing with such a situation, N objective functions are accordingly required as $f_j(\mathbf{p}_j, \mathbf{g})$. It is highly desirable that the optimized gap function $g(\mathbf{x})$ would have all the objectives $f_j(\mathbf{p}_j, \mathbf{g})$ ($j = 1, 2, \dots, N$) being minimized. Thus the shape optimization of the contact system subjected to the multiple load cases can be defined as,

$$\begin{cases} \min f(g(\mathbf{x})) = \min [f_1(\mathbf{p}_1, \mathbf{g}), f_2(\mathbf{p}_2, \mathbf{g}), \dots, f_N(\mathbf{p}_N, \mathbf{g})]^T, \\ \text{s.t. } g^L(\mathbf{x}) \leq g(\mathbf{x}) \leq g^U(\mathbf{x}), \end{cases} \quad (4)$$

where $g^L(\mathbf{x})$ and $g^U(\mathbf{x})$ stand for the lower and upper bounds of the contact gap function respectively.

However, it is hardly possible to achieve such N design criteria simultaneously. It is found that to some stage, any further improvement in one criterion requires a clear tradeoff with at least one other criterion. This defines a Pareto optimum [35], where there exists no feasible solution $g(\mathbf{x})$ that can decrease some objective functions without causing at least one objective function to increase. In this sense, the Pareto optimum represents a range of solutions. Indeed, only can the solution to the optimization subjected to multiple load cases be laid on a Pareto implication.

To obtain some form of the Pareto optimum solutions to design problems under multiple load cases, numerous methods can be adopted [1,36–38]. One of the easiest approaches is to construct a single cost function which can appropriately reflect the major design requirement.

3.1. Extreme stress criterion

One of most popular approaches to the treatment of multiple load conditions is to identify the most critical load case. For this purpose, when the system, under multiple load conditions, is solved, the highest stress level over all loadings is usually given priority [19,37]. The design goal would be to reduce the contact stress peak in the worst loading case as

$$\hat{f}(g(\mathbf{x})) = \max_j [f_1(\mathbf{p}_1, \mathbf{g}), f_2(\mathbf{p}_2, \mathbf{g}), \dots, f_j(\mathbf{p}_j, \mathbf{g}), \dots, f_N(\mathbf{p}_N, \mathbf{g})]. \quad (5)$$

In favor of this design criterion, Eq. (2) is adopted as the sub-objective function corresponding to each load case,

$$f_j(\mathbf{p}_j, \mathbf{g}) = \max_i [\sigma^1(\mathbf{p}_j, \mathbf{g}), \sigma^2(\mathbf{p}_j, \mathbf{g}), \dots, \sigma^i(\mathbf{p}_j, \mathbf{g}), \dots, \sigma^M(\mathbf{p}_j, \mathbf{g})], \quad (6)$$

where $\sigma^i(\mathbf{p}_j, \mathbf{g}) \equiv \sigma_j^i$ denotes the contact stress at the i th contact node under the j th load case. Substitution of Eq. (6) into (5), the following relation holds

$$\hat{f}(g(\mathbf{x})) = \max_j \left\{ \max_i [\sigma^i(\mathbf{p}_j, \mathbf{g})] \right\} = \max_i \left\{ \max_j [\sigma^i(\mathbf{p}_j, \mathbf{g})] \right\}. \quad (7)$$

Hence, the highest contact stress at the i th contact node pair over all load cases ($j = 1, 2, \dots, N$), can be taken as the *extreme reference stress* as

$$\tilde{\sigma}^i = \max_j [\sigma^i(\mathbf{p}_j, \mathbf{g})] = \max_j [\sigma^i(\mathbf{p}_1, \mathbf{g}), \sigma^i(\mathbf{p}_2, \mathbf{g}), \dots, \sigma^i(\mathbf{p}_N, \mathbf{g})]. \quad (8)$$

Eq. (7) can be accordingly re-expressed as

$$\bar{f}(g(\mathbf{x})) = \bar{\sigma}^{\max} = \max_i \bar{\sigma}^i = \max_i \left\{ \max_j [\sigma^i(\mathbf{p}_j, g)] \right\}, \tag{9}$$

where $\bar{\sigma}^{\max}$ denotes the highest reference stress over all the contact nodes.

Such a design criterion can result in an even distribution of the extreme stress level over all the load cases. That is to say, the modification of the nodal gap depends only on the maximum or most influential load case at each node. From a static strength point of view, this appears an adequate criterion, where an “immediate” surface failure may rely heavily on the highest contact stress level.

3.2. Weighted average criterion

It is clear that, in the extreme stress criterion, the effect of other lower stress cases on a specific contact node pair is completely disregarded. Under some circumstances, such a critical load case may be applied for a very short duration or have little importance. In contact fatigue or surface wear design, the failure could depend, not only on the magnitude of a stress, but also on the operational frequency or service duration. The extreme scheme does not seem a convincing way to account for failure due to contact fatigue or wear. To accommodate this situation, the weighted average criterion is introduced herein.

For simplicity, it is assumed that the weight coefficient $w_j(\mathbf{p}_j) \geq 0$ corresponding to the j th load case is allocated in a constrained form of

$$\sum_j w_j(\mathbf{p}_j) = 1. \tag{10}$$

Thus a unified objective function can be constructed as

$$f_u(g(\mathbf{x})) = \mathbf{w}^T \cdot \mathbf{f} = \sum_j w_j(\mathbf{p}_j) f_j(g(\mathbf{x})). \tag{11}$$

From the definition of the objective function as in Eqs. (2), (11) can be further written as,

$$f_u(g(\mathbf{x})) = \sum_j w_j(\mathbf{p}_j) \sigma_j^{\max} = \sum_j \max_i [w_j(\mathbf{p}_j) \sigma_j^i]. \tag{12}$$

It can be seen that Eq. (12) does not explicitly provide any reference to individual node. To facilitate the ESO procedure, however, it is indispensable to establish the nodal references [23–25]. For this purpose, one of the typical approaches is to formulate a *weighted reference nodal stress* in an alternative way as in references [19,39,40],

$$\bar{\sigma}^i = \sum_j w_j(\mathbf{p}_j) \sigma_j^i \tag{13}$$

which represents the weighted sum of the contact stresses at node i over all the load cases. Obviously, Eq. (12) presents an upper bound of the weighted reference stress $\bar{\sigma}^i$ in Eq. (13), i.e.

$$f_u(g(\mathbf{x})) \equiv \sum_j \max_i [w_j(\mathbf{p}_j) \sigma_j^i] \geq \max_i \bar{\sigma}^i \equiv \max_i \left[\sum_j w_j(\mathbf{p}_j) \sigma_j^i \right]. \tag{14}$$

Similarly to Eq. (9), let $\bar{\sigma}^{\max}$ stand for the maximum value of the weighted reference contact stress (13). And an alternative objective function can be consequently expressed as

$$\bar{f}(g(\mathbf{x})) = \bar{\sigma}^{\max} = \max_i \left[\sum_j w_j(\mathbf{p}_k) \sigma_j^i \right] = \max_i [\bar{\sigma}^1, \bar{\sigma}^2, \dots, \bar{\sigma}^i, \dots, \bar{\sigma}^M]. \tag{15}$$

It is evident that the weight coefficients provide a means of dealing with various load cases differently. For instance, the weights can be employed to reflect the operational frequency of any load case (i.e. the time the loads are applied for) or to emphasize the importance of one load case relative to another. Apparently, such a scheme presents an overall measure to all the load cases, where the effect of every load case is taken into account in the sense of a weighted average [18,19]. More importantly, by varying the weights it is also possible to generate the Pareto optimal solution [1,38], which puts the designer into a better position as a decision maker by showing the optimal set other than a single optimum point.

In real world, different load cases may lead to considerably different objective magnitudes. For convenience, some forms of normalization of the objective functions can be introduced as discussed in the literature [1]. It is expected that the normalization can noticeably reflect the uniformity of the reference stress. One of the typical methods is to map the original objective function, Eq. (9) or (15), as,

$$f(g(\mathbf{x})) = \frac{\bar{f}_k^{\max} - \bar{f}_k^{\min}}{\bar{f}_0^{\max} - \bar{f}_0^{\min}} = \frac{\tilde{\sigma}_k^{\max} - \tilde{\sigma}_k^{\min}}{\tilde{\sigma}_0^{\max} - \tilde{\sigma}_0^{\min}}, \tag{16}$$

where subscript k stands for the number of the iteration and $\tilde{\sigma}^{\min}$ denotes the minimum value of all the reference stresses as

$$\tilde{\sigma}^{\min} = \min_i [\tilde{\sigma}^1, \tilde{\sigma}^2, \dots, \tilde{\sigma}^i, \dots, \tilde{\sigma}^M]. \tag{17}$$

It is found that Eq. (16) can make the different design problems and criteria more comparable. Hence, it is adopted as the normalized objective function in this paper.

4. An evolutionary approach to optimization of gap shape

One of the most efficient approaches to redistribute the contact stress could be to directly modify the contact interfaces [23–25,31–34]. That is to say that the gap $g(\mathbf{x})$ can be treated as design variables. It is generally recognized that separating a pair of corresponding contact nodes would make the contact stresses between them decrease. When using gap elements to model the contact system, this can be simply implemented by adjusting the gap spacing between the pair of contact nodes. Thus, the gap elements between the corresponding nodes on both surfaces are used not only to model contact states but also to modify the contact profile by changing the spacing to lengthen or shorten the gap between the corresponding nodes. However, due to the highly nonlinear nature of the problem, it is difficult to find optimal gap spacing over the whole contact surface in any one single analysis-design cycle. Hence, the optimization process needs to be accomplished in an iterative manner.

In each iteration, the elastic contact finite element analysis is performed for each load case and subsequently the distributions of reference contact stresses at the interfaces are determined, as Eqs. (8) and (13). If the normalized objective function (16) does not fall within a prescribed convergence tolerance, the relative reference stress level of each contact node is computed by comparing with the maximum or mean reference contact stress (i.e. $\tilde{\sigma}^i/\tilde{\sigma}^{\max}$ or $\tilde{\sigma}^i/\tilde{\sigma}^{\text{avg}}$). Based on such relative stress levels, the contact profile is modified by changing the coordinates of the corresponding contact node pairs. The modification can be performed by increasing the gap spacing between the node pairs that have higher relative reference stress levels. Clearly, the ESO method is different from the traditional evolutionary algorithms that were directly inspired from Neo-Darwinian hypothesis. Instead, ESO reflects an evolutionary adaptation or modification process of systems within a specific environment (e.g. multiple load cases herein) [16].

Mathematically, the present evolutionary modification amount is computed as a function of the relative reference contact stress level of the nodal pair over the contact interface as,

$$\hat{\Delta}^i = fn\left(\frac{\tilde{\sigma}^i}{\tilde{\sigma}^{\max}}\right)\mathbf{n}^i, \tag{18}$$

where $\hat{\Delta}^i$ is the current gap modification vector at the i th node pair, \mathbf{n}^i the normal vector at the node of the design interface.

For simplicity, in this paper, a power law with a constant coefficient MR is adopted to control the *Modification Rate* as

$$\Delta^i = \text{MR} \times \left(\frac{\tilde{\sigma}^i}{\tilde{\sigma}^{\max}} \right)^r \mathbf{n}^i \quad (19)$$

which is of a similar form to the typical ESO procedure [15,16] except a more general exponential scaling scheme. In this paper, the second order power ($r = 2$) is set for the demonstrative examples.

However, it should be pointed out that Eq. (19) may lead to gap function $g(\mathbf{x})$ keep increasing as the iteration progresses. In other words, $g(\mathbf{x})$ would converge to a stage that contains a certain amount of constant translation from its initial status. To compute the relative modification of the gap at each iteration, Eq. (19) is modified as

$$\Delta^i = \text{MR} \times \left(\frac{\tilde{\sigma}^i}{\tilde{\sigma}^{\max}} - \frac{\tilde{\sigma}^{\min}}{\tilde{\sigma}^{\max}} \right)^r \mathbf{n}^i \quad (20)$$

in which the unnecessary increase in the gap is filtered.

To enhance the computational efficiency, the modification can also be carried out in a *bi-directional* fashion, either increasing the gap spacing for a highly stressed contact pair or decreasing the gap spacing (when feasible) for a lowly stressed contact pair. This can be formulated as

$$\Delta^i = \text{MR} \times \text{sgn}(\tilde{\sigma}^i - \tilde{\sigma}^{\text{avg}}) \left| \frac{\tilde{\sigma}^i - \tilde{\sigma}^{\text{avg}}}{\tilde{\sigma}^{\text{avg}}} \right|^r \mathbf{n}^i, \quad (21)$$

where $\tilde{\sigma}^{\text{avg}}$ denotes the mean reference stress level over the design contact region and can be computed as

$$\tilde{\sigma}^{\text{avg}} = \frac{1}{A_C} \int_{A_C} \tilde{\sigma}(g(\mathbf{x})) dA_C, \quad (22)$$

where A_C denotes the area of contact region and $\tilde{\sigma}$ the reference contact stress. Based on the step modification of gap spacing, the gap vector of the contact pair can be updated as,

$$\mathbf{g}_k^i = \mathbf{g}_{k-1}^i + \Delta_k^i \quad (23)$$

or the coordinates of the corresponding design boundary as,

$$\mathbf{x}_k^i = \mathbf{x}_{k-1}^i + \Delta_k^i, \quad (24)$$

where subscript k stands for iteration step of the evolutionary procedure and \mathbf{g}^i the current gap spacing vector for contact pair i .

It should be noted that the gap beam length would change with the coordinate modification of the nodes at both its ends. As mentioned in the FEA contact modeling, the initial length of the gap element indicates the critical contact state. To implement this concept into the whole optimization process, a virtual thermal strain is introduced to the gap element whose nodes need modifying. Taking a pair of nodes (i_1, i_2) with higher stress level as an example, the coordinate of node i_1 is moved apart from i_2 with a step length of Δ_k^i as shown in Fig. 2. In order to make the gap beam element contract in length equal to this coordinate modification, a fictitious tensile stress is introduced by giving the nodes at both ends of the gap beam element a temperature T^i (less than the reference temperature T_{ref}^i) to provide a total tensile deformation of \mathbf{g}_k^i . This can be done by satisfying the equation,

$$\alpha(T^i - T_{\text{ref}}^i)L^i \mathbf{n}^i = -\mathbf{g}_k^i, \quad (25)$$

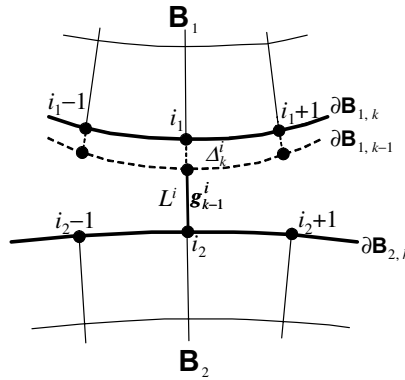


Fig. 2. Gap modification.

where L^i is the initial length of the i th gap element and α the coefficient of thermal expansion of the gap beam material.

According to the nature of the compressive-only gap element, it will act only when the compressive stress becomes larger than this fictitious tensile stress. In the subsequent iteration, therefore, the tensile pre-stressed beam element will be ignored by the FE solver during the first few iterations until the load or deformation is big enough to cause the modified gap g^i to close and the beam element goes into compression.

To judge the convergence of design objective, a tolerance τ needs to be prescribed. In this study, a relative change in the normalized objective function (16) is checked in two successive iterations (the $(k - 1)$ th and the k th) as

$$\left| \frac{f_k(g(\mathbf{x})) - f_{k-1}(g(\mathbf{x}))}{f_k(g(\mathbf{x}))} \right| \leq \tau. \tag{26}$$

A value of $\tau = 0.01\%$ is adopted in the demonstrative examples of this paper.

For clarification, the main steps of the evolutionary optimization process for the multiple load cases can be systematically reorganized as follows:

- Step 1: Set up a contact finite element model and impose multiple load cases. Determine the ESO design criterion; Set up the ESO driven parameters: the modification rate MR and convergence tolerance τ ;
- Step 2: Carry out finite element contact analyses for individual load cases as given in Eq. (1);
- Step 3: Calculate the nodal reference stress level according to either (8) or (13);
- Step 4: Compute the objective function f_k as (16);
If convergence criterion (26) is satisfied, terminate the iteration and output the results of optimization. Otherwise go to Step 5;
- Step 5: Modify the gap spacing (23) in terms of the relative levels of nodal reference contact stresses as (20) or (21);
- Step 6: Update the nodal coordinates according to (24) and remesh the grid of the design domain whenever necessary. Set $k = k + 1$ and go back to Step 2.

A batch file is set up to automatically carry out the iteration cycles of the multiple finite element analyses, computations of nodal reference stress, contact gap modifications and re-meshing in order to make the objective function f gradually decrease and eventually meet the optimality criteria.

5. Demonstrative examples

To demonstrate how the proposed ESO procedure optimizes the contact profiles for the structures subject to multiple load cases, three illustrative examples are presented herein: (1) elastic to rigid body contact without friction; (2) elastic to elastic non-frictional contact and (3) elastic to elastic frictional contact.

5.1. 2D elastic-rigid contact subjected to two load cases

A rectangular elastic plate on a rigid foundation is subjected to two separate load cases, $p_1 = 1N$ and $p_2 = 1N$, as illustrated in Fig. 3. In the ESO processes, both the extreme stress and the weighted average criteria are considered. A modification rate of $MR = 0.2\%$ is set for all design cases in this example.

When the extreme stress criterion is adopted, the higher nodal contact stress under p_1 and p_2 is used for the modification of the initial gap. As a result of the optimization, the higher stress levels for both load cases finally become uniform as shown in Figs. 4(b) and 5(b). By comparing to the initial designs as depicted in Figs. 4(a) and 5(a), one can easily identify the significant reduction in the extreme stress levels (by around 55%). At the same time, the contact stress peak for any individual load case is remarkably “cut” off too.

It is worth pointing out that, in such a situation, the lower stress level under both the load cases is completely disregarded. Moreover, the stress distribution for any individual load case is noticeably non-uniform

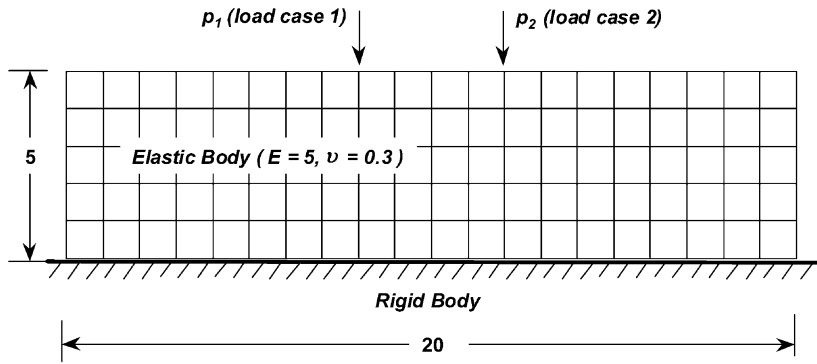


Fig. 3. Finite element model of structure under multiple load case.

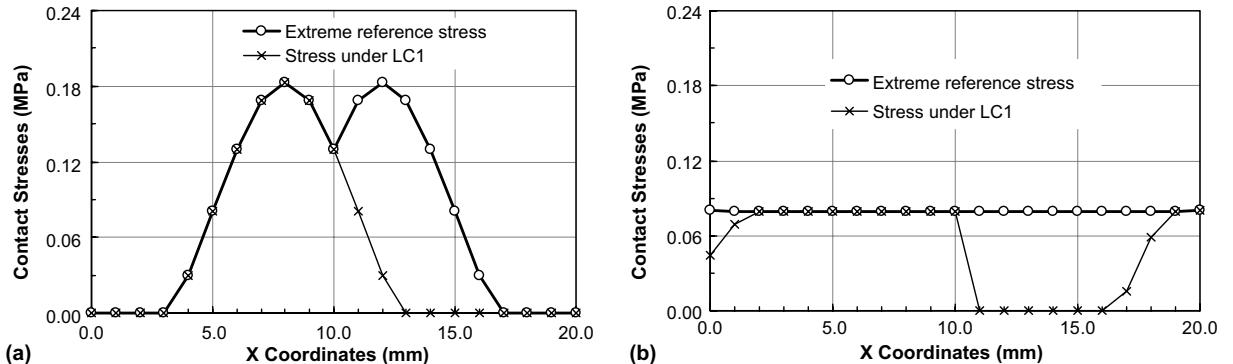


Fig. 4. Distributions of the contact stresses under load case 1 (extreme stress criterion): (a) Initial design and (b) final design.

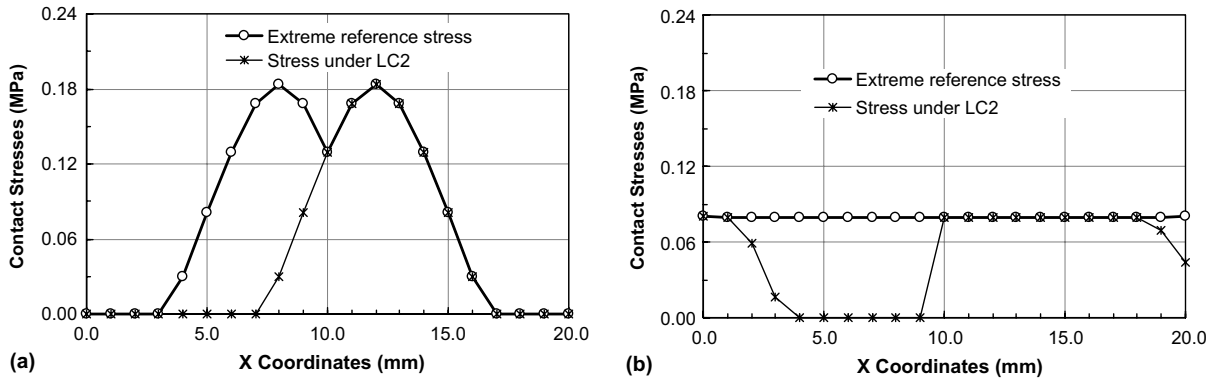


Fig. 5. Distributions of the contact stresses under load case 2 (*extreme stress criterion*): (a) Initial design and (b) final design.

for even the final design (observe Figs. 4(b) and 5(b)). Indeed, if one considers either of the load cases (for example, load case 1 in Fig. 4), it is found that, in the final design, the contact stresses of some contact pairs reach the highest level while others may even not be in contact (i.e. zero stress). However, when looking at both the load cases, it can be seen that the higher stress level at any contact pair becomes identical. This means that the design is optimal only in a sense of the extreme stress criterion. In other words, the average stress level over the interfacial contact nodes may not be equal.

When the weighted average criterion is applied, the nodal *average* contact stresses under both load vectors p_1 and p_2 are considered prior to the modification of the initial gap. For the illustrative purpose, in this example, an even allocation of the weighing coefficients is given as,

$$w = w_1(p_1) = w_2(p_2) = 0.5. \tag{27}$$

This may reflect that there is an identical emphasis on both load cases or/and both the load cases have equal operation frequency.

Similarly to the extreme stress criterion, for the weighted average criterion, the peaks of the *reference stress* and the individual stress are eliminated by comparing Figs. 6(b) with 6(a) and 7(b) with 7(a). The final distribution of the average contact stresses becomes uniform as shown in Figs. 6(b) and 7(b).

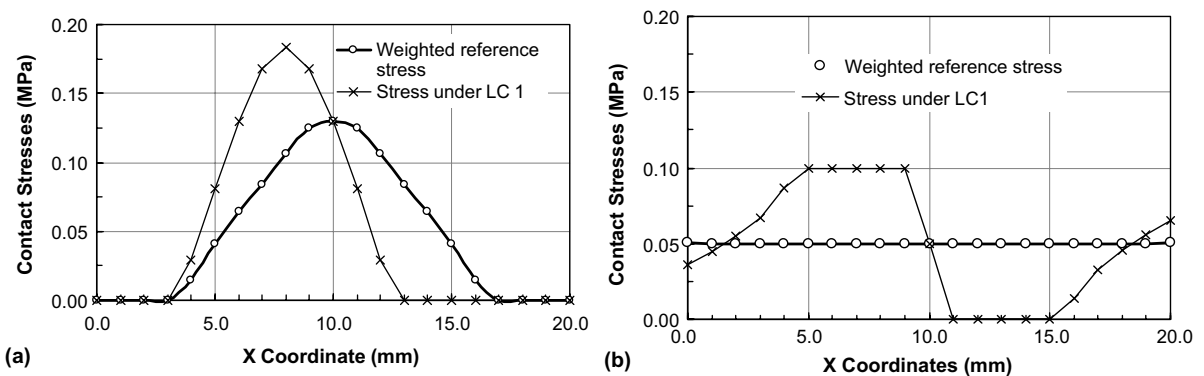


Fig. 6. Contact stress distributions for load case 1 (*weighted average criterion*): (a) Initial design and (b) final design for load case.

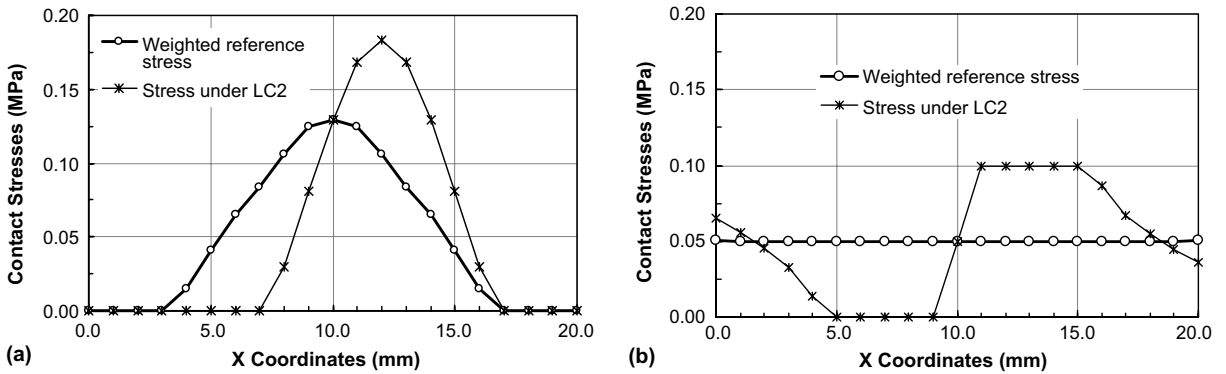


Fig. 7. Contact stress distributions for load case 2 (weighted average criterion): (a) Initial design and (b) final design.

However, the contact stress distribution for any individual load case is also uneven, as shown in Figs. 6(b) and 7(b). This indicates that the design is an optimum for both the load cases, only in a sense of the weighted average criterion. It is worth noting that the effect of the lower stress level of each contact pair has been regarded in this criterion. From Figs. 6 and 7, it is interesting to notice that the stress distributions appear symmetric in relation to the central line of the structure. This is due to the symmetry of the loading location of load cases 1 and 2.

By comparing Figs. 4, 5 with Figs. 6, 7, it is found that, in this specific example, the highest nodal stress under the extreme criterion is lower than that under the weighted average criterion (i.e. 0.08 vs 0.10). But the average nodal stress under the extreme criterion is higher than that under the weighted average criterion (0.075 vs 0.050). This clearly reveals that the different criteria do produce different optimal outcomes.

The convergence indices for the both design criteria are plotted in Fig. 8. It is interesting to note that the convergence rate for the weighted average criterion is faster than that for the extreme stress criterion. This may be accounted in that the initial distribution pattern for the weighted average criterion is somewhat simpler (with a single convex peak) than that of the extreme stress case (with double convex peaks). In this figure, it can be observed that three noticeable oscillations appear in both the convergence curves. This is also a result of the three isolate “zero reference stress points” of the objective functions in each side

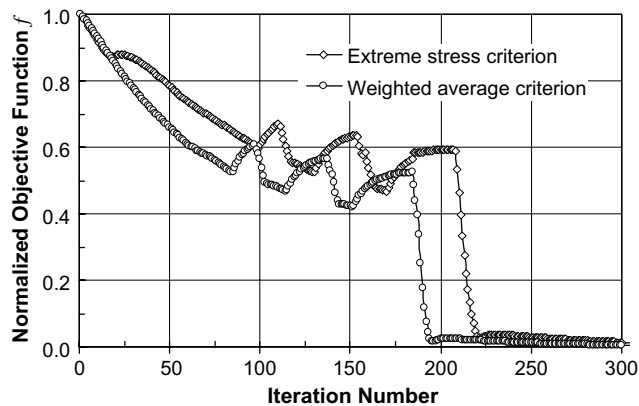


Fig. 8. Convergence index for the both criteria.

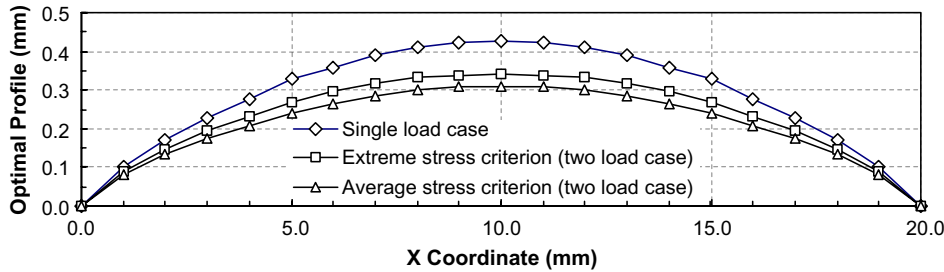


Fig. 9. The comparison of optimal contact profiles under different criteria.

of the contact interface, as shown in Figs. 4(a), 5(a) and 6(a), Fig. 7(a), which has been thoroughly investigated by the authors [23].

The difference between the optimal contact shapes under both criteria can be seen in Fig. 9. It is observed that, in this example, the optimal gap under the weighted average criterion is smaller (flatter) than that under the extreme stress criterion. This provides more evidence that the gap modification for the weighted average criterion appears somewhat easier to be achieved than that for the extreme stress criterion because averaging in both the stresses makes the objective stress distribution simpler and smoother. In contrast, since more compromise or trade-off is required for the extreme stress criterion method, the gap modification becomes more difficult. Therefore, more modification is involved before reaching an optimum.

To compare the difference between the single load case and the multiple load cases, an analysis is also carried out for a situation where both p_1 and p_2 are applied simultaneously, i.e. a single load case consisting of two point loads. The optimal gap allocation of the single load case is obviously greater than that of the multiple load cases, as shown in Fig. 9. One of the main reasons is that the total force in the single load case is as twice as that in the multiple load cases. This shows another feature in the contact design that the higher the external load, the greater the optimal gap.

5.2. 2D elastic–elastic contact subjected to two load cases

The contact between two elastic bodies is studied in the second example. As shown in Fig. 10, two distributed load cases p_1 and p_2 are separately applied on the top edge of the upper elastic body. For simplicity, only the upper body is treated as the design domain. A modification rate of $MR = 2\%$ is set for all design cases in this example.

From the previous example, it seems that the weighted average criterion offers more flexibility than the extreme stress one. The choice of the weight coefficients enables designers to deal with various load conditions differently. In design process, this would be convenient when one or several load cases need to be especially emphasized.

In order to observe the results of the extreme stress criterion in this example, Fig. 11(a) and (b) respectively depict the initial and final contact stress distributions with the extreme stress criterion. It can be seen that the “corner effect” of the objective stress in the initial design is completely removed in the final one (Fig. 11(b)). Moreover, the highest contact stresses for both the load cases become uniform in this criterion. However, it can be seen that, in the final design, the lower stresses near the central area are considerably greater than those near the edges. This reflects that, in an overall sense, the usage efficiencies of central contact pairs are higher than those of edge ones. In other words, the contact pair in the central area may experience a more intensive contact stress level. To deal with such a situation, the weighted average criterion is also considered for this example below.

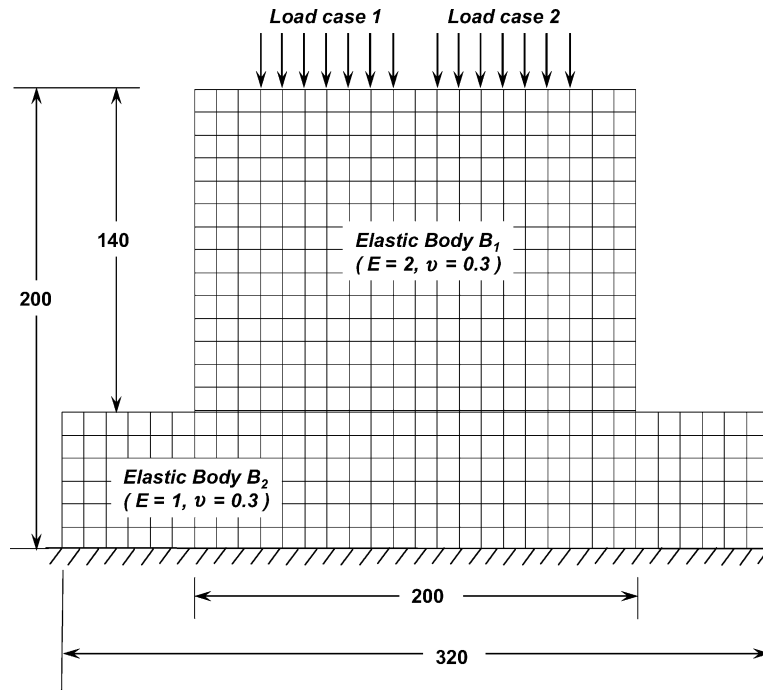


Fig. 10. Finite element modelling of elastic-elastic contact.

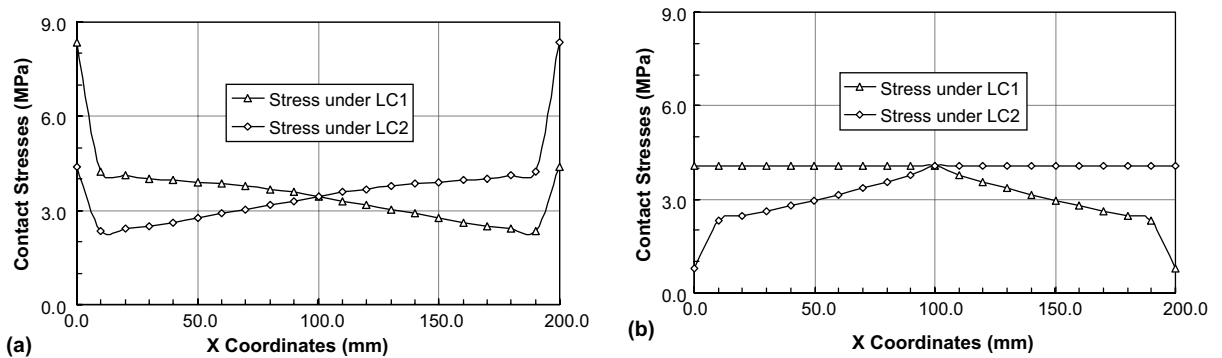


Fig. 11. Contact stress distribution for the extreme stress criterion. (a) Initial design and (b) final design.

The weighted average criterion provides a substantial measure to the overall stress level. It also offers the convenience and the flexibility to cope with various load cases differently. In this example, five allocation schemes of weights are taken into account as

$$\text{Case A: } w_1(\mathbf{p}_1) = 1.00 \text{ and } w_2(\mathbf{p}_2) = 0.00, \tag{28}$$

$$\text{Case B: } w_1(\mathbf{p}_1) = 0.75 \text{ and } w_2(\mathbf{p}_2) = 0.25, \tag{29}$$

$$\text{Case C: } w_1(\mathbf{p}_1) = 0.50 \text{ and } w_2(\mathbf{p}_2) = 0.50, \tag{30}$$

Case D: $w_1(\mathbf{p}_1) = 0.25$ and $w_2(\mathbf{p}_2) = 0.75$, (31)

Case E: $w_1(\mathbf{p}_1) = 0.00$ and $w_2(\mathbf{p}_2) = 1.00$. (32)

In effect, Cases A and E represent single load cases, Case C gives an even allocation of the weights and Cases B and D are employed to treat these two load cases differently.

Fig. 12 shows the contact stress distributions for the different allocations of the weights. Taking Fig. 12(b) as an example (Case B: $w_1 = 0.75$ and $w_2 = 0.25$), a larger weight is given to the load case 1 ($w_1(\mathbf{p}_1) = 0.75$). As a result of this, the contact stress distribution of load case 1 appears considerably flatter than that of load case 2, as shown in Fig. 12(b). This means that the contact stresses under load case 1 are controlled more. In other words, load case 1 has played a dominant role in the design process and thus the distribution of the corresponding stress becomes more uniform. A similar result can also be observed in Fig. 12(a). Similarly to the previous example, an equal allocation of weights ($w_1(\mathbf{p}_1) = 0.50$ and $w_2(\mathbf{p}_2) = 0.50$) may represent an identical emphasis on both load cases, and as a result, the corresponding optimal stress distributions are symmetric, as shown in Fig. 12(c).

Fig. 13 depicts the effects of the two design criteria as well as the weights on the final design shapes. Similarly to the preceding example, it can be seen that the gap with the extreme stress criterion is greater than that with the 50%:50% weighted average criterion. As predicted, in the weighted average criterion, the weight allocation of 25%:75% gives a symmetrical gap distribution to that of 75%:25%. It is observed that the optimal gaps corresponding to a heavier weight are larger. Still taking Case B ($w_1 = 0.75$ and $w_2 = 0.25$)

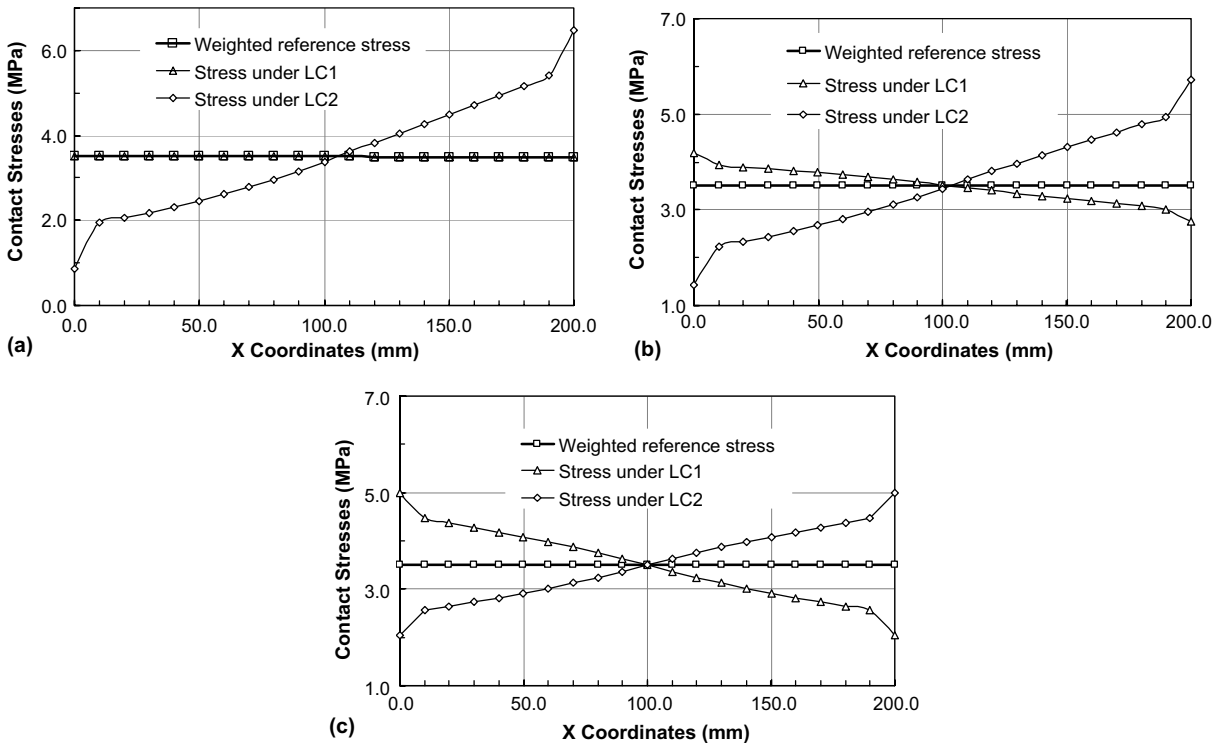


Fig. 12. Optimal contact stress distribution for the weighted average criterion: (a) Case A: $w_1(\mathbf{p}_1) = 1.00$ and $w_2(\mathbf{p}_2) = 0.00$, (b) Case B: $w_1(\mathbf{p}_1) = 0.75$ and $w_2(\mathbf{p}_2) = 0.25$ and (c) Case C: $w_1(\mathbf{p}_1) = 0.50$ and $w_2(\mathbf{p}_2) = 0.50$.

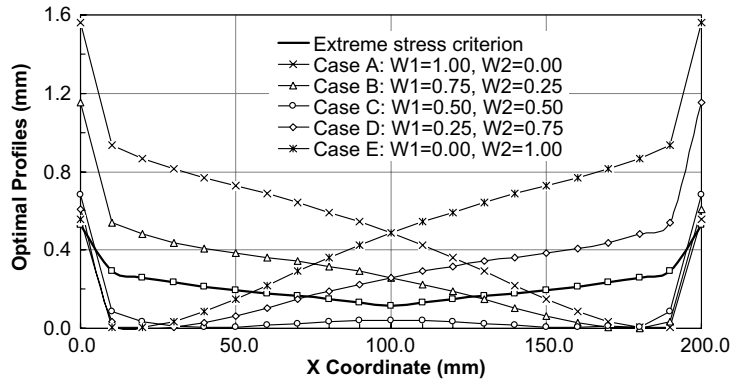


Fig. 13. Comparison of optimal gaps between various weights and design criteria.

as an example, the contact gap in the right end is considerably smaller than that in the left end. This is because a heavier emphasis has been placed on load case 1 (75%, on the left). In other words, load case 1 plays a more important role in the design process. As a result, a major gap modification has been carried out over the left side of the contact region where load case 1 is applied.

From the above discussion, it is evident that the selection of the weights is a crucial step in design process. However, it is usually difficult to know or fix in advance. Thus it seems appropriate to allocate the right weights in a trial-and-error fashion during the design. As a consequence of this, a set of Pareto optima can be produced using varying weights. Fig. 14 depicts the evolutionary processes for Cases A–E in detail. As the design progresses, it is seen that both the objectives, f_1 and f_2 are getting improved. However, the further improvement will be impossible after converged. These several converged points (as marked in A, B, C, D and E) are interpolated into a sketch of the Pareto frontier in the design space as shown in Fig. 14. It is known that in the Pareto frontier, there exists no feasible solution that can decrease one objective function without causing other objective functions to increase. In other words, once one Pareto optimum (corresponding to a set of weights, e.g. $w_1 = 0.75$ and $w_2 = 0.25$) is achieved, any further improvement

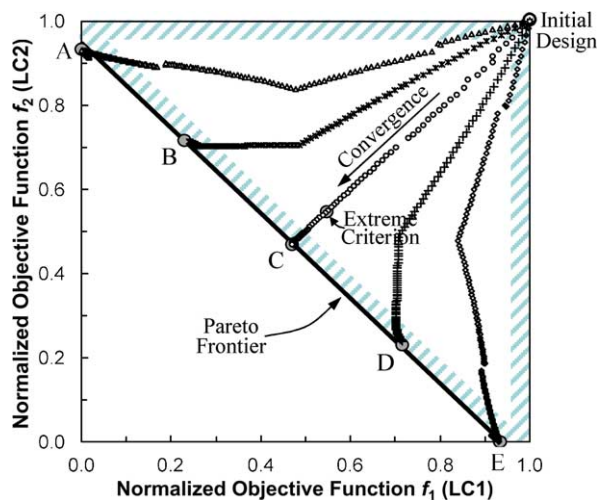


Fig. 14. Optimization processes and the Pareto frontier for the multiple load cases.

in one objective function requires a clear tradeoff with the other objective. This is one of the advantages of the weighted average criterion, in which the designer has a better chance to understand the entire Pareto solution space.

In addition, it is interesting to note that the solution based on the extreme stress criterion does not represent a Pareto solution in this example as illustrated in Fig. 14, which appears consistent with the observations by Proos et al. [36]. This implies that in a Pareto sense, the extreme stress criterion (or the *worst case design*) would not always yield a “best possible” solution to the prescribed objective in spite of its practical significance in engineering design. That is to say that the designer could actually find a better solution than this one from a less conservative point of view. In this example, for instance, the design with a 50%:50% allocation of the weights does give a considerable better solution to both the objectives. As a consequence of this example, producing a Pareto solution space would be always helpful for making a best possible decision whenever achievable.

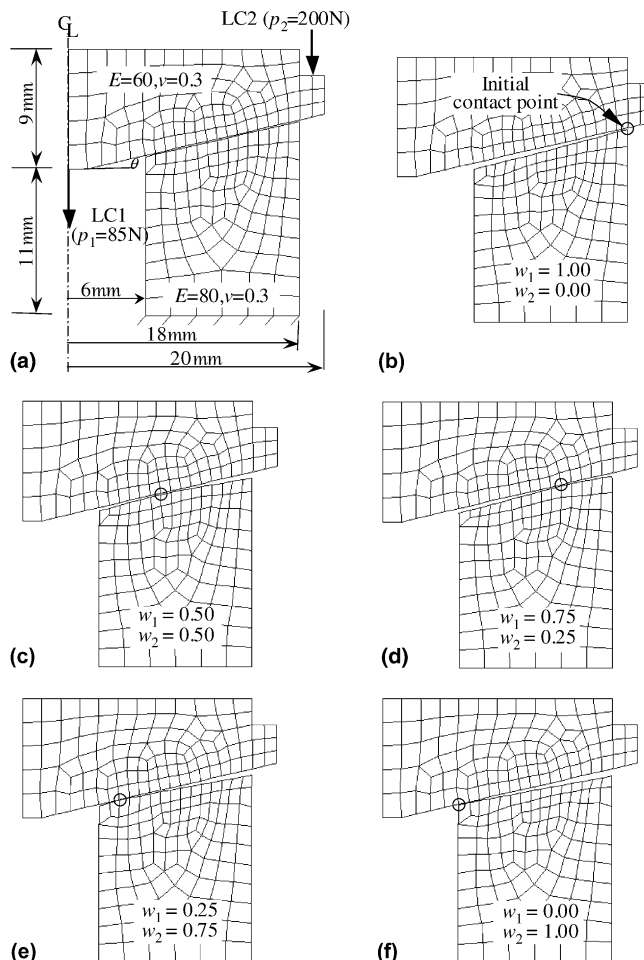


Fig. 15. Frictional contact shape optimization of axisymmetrical cone-on-socket problem. (a) Initial design, (b) Case A, (c) Case B, (d) Case C, (e) Case D and (f) Case E.

5.3. Frictional axisymmetrical contact design with multiple load cases

Due to the ideal self-alignment feature, conical spinning joints are very common in a wide range of engineering applications, e.g. thrust bearings, automotive valve-on-seat, friction clutches and conical brakes [41]. One question with great practical importance is how to design the mating contact surfaces to reduce wear of these elements as much as possible.

In those two preceding plane-stress examples, friction effect has not been considered and the design surfaces are simply parallel to the reference axis and perpendicular to the external loads. This current example will demonstrate the capability of the ESO method in solving more practical problems, where both friction and inclined design surface (with a conical angle $\theta = 12.5^\circ$) are taken into account for axisymmetric problem under multiple load cases.

Shown in Fig. 15(a) is the FE model of the initial design, where two load cases p_1 and p_2 are axially applied in the central and flange regions. Different from the above examples, the lower elastic body (i.e. the socket) is selected as the design domain in this example. In the ESO procedure, a modification rate of $MR = 0.5\%$ is set for all design cases in this example. Considering that the wear is the major concern of this kind of problems, only a weighted average criterion is adopted herein, which facilitates a wear rate computation as in [41].

As before, an evenly distributed set of weights is adopted for approximately estimating Pareto's space for both frictional and non-frictional contact designs. Figs. 15(b)–(f) present the optimal gap designs for the frictional conical joint in several sets of weight allocations. It is interesting to observe that a nearly straight line appears in Case A (Fig. 15(b)) and Case E (Fig. 15(f)), which respectively corresponds to the two special scenarios with single load case (wherein: $w_2 = 0.00$ or $w_1 = 0.00$). This seems to excellently correlate to the traditional conical designs [41]. However, the other allocations of the weights produce various convex curves with the initial contact points moving from the outer radius to inner radius as w_1 decreases and w_2 increases, Fig. 15(b)–(f).

To better compare Pareto curves of the frictional design with the non-frictional design, a non-normalized objective, which is given as the deviation of the maximum and minimum contact stresses, is adopted for plotting Fig. 16. It can be clearly seen that in Pareto sense, the non-frictional design is fairly worse than the frictional design in this example. In the frictional design, the contact traction consists of normal and

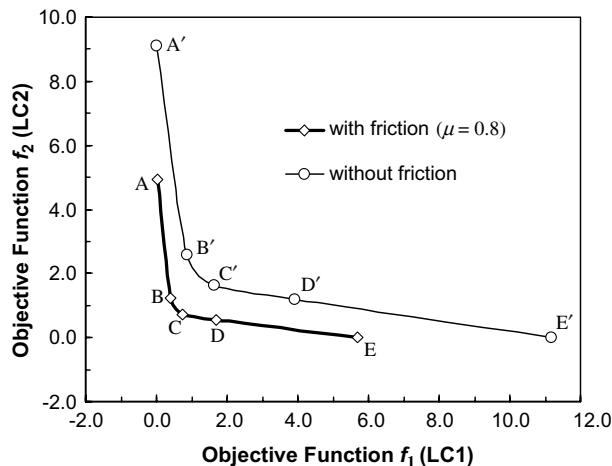


Fig. 16. Pareto curves for the frictional and non-frictional contact design problems.

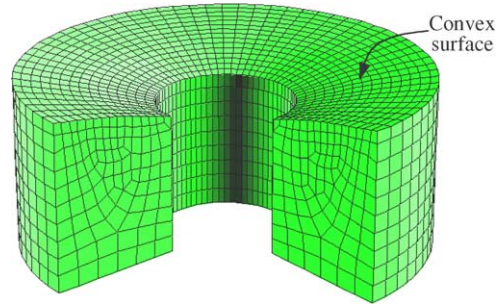


Fig. 17. Sketch of optimal design of frictional surface ($w_1 = w_2 = 0.50$).

tangential components, which can considerably affect the design processes. The noteworthy difference indicates that the negligence of friction may lead to a worse design in multiple load cases.

Fig. 17 shows a 3D sketch of curved upper surface in the socket with an equal allocation of the weights. It should be pointed out that the gap modification has been performed along normal directions of design surface as described in Eq. (20), which may keep changing as the design progresses. From manufacturing point of view, in addition, such convex optimized surfaces (also refer to Fig. 13) seems more appropriate than the concave surfaces as presented in the first example (Fig. 9) during machining and grinding. Having given normal contact gap as design variables, the ESO method is particularly flexible in coping with different design domains and manufacturing requirements.

6. Concluding remarks

This paper presents a new enhancement to the ESO method for elastic contact optimization, where the multiple load case problems are taken into account. Unlike the single load case, the multiple load conditions may be reflected in terms of the different design criteria. In this paper, two unified schemes are presented to incorporate the effects of the multiple load cases into the design process.

In the extreme stress criterion, the highest stress level is considered as the reference criterion, while in the weighted average criterion, a weighted overall stress is regarded as reference level. These two different criteria may provide the designers with different results. In the extreme stress criterion, all lower stress levels are completely ignored in the design process. Sometimes, this may not appropriately reflect the real loading situation at all contact pairs. Conversely, the lower stress levels are taken into account in the weighted average criterion. The adoption of weights offers a superior possibility to place greater emphasis to some load conditions in terms of its importance or operational frequency.

Three design examples are presented to demonstrate the effectiveness and the capability of ESO in this paper. These two design criteria are compared in detail from the first two illustrative examples. It is observed that the extreme stress criterion (the worst case design) may not always locate in the Pareto frontier. The effect of friction on the Pareto frontiers is also investigated in the third example. It is found that the negligence of friction in the contact design with multiple load cases may result in a non-optimal Pareto frontier.

Five sets of equal weight allocations have been used to provide a sketch to the shapes of Pareto curves in the last two examples. Both sketches approximately indicate a predictable convexity in Pareto space, which reflects a successful use of linear weight average method in these two contact design examples. In addition, it is interesting to note that the scheme of evenly distributed sets of weights may result in an almost uniform spread of Pareto point in some cases (e.g. the second example), but not in others (e.g. the third example).

This implies that an even spread of Pareto points may require a more sophisticated scheme of allocating the weights. As pointed out by Das and Dennis [40], nevertheless, such an equal-weighted draft can be an important step before establishing a more appropriate weight allocation scheme. An in-depth discussion of this problem is beyond the scope of this study and can be found from literature [38,42,43]. It is advisable for a designer to begin with a sketch of a Pareto frontier in the design problems before a more detailed and more systematic depiction is carried out.

Acknowledgment

The second author is supported by Australian Research Council (ARC) under the Fellowship scheme (F00105542). Also, the authors are grateful to the anonymous referees for their valuable comments and constructive suggestions on the early version of this manuscript.

References

- [1] M. Papadrakakis, N.D. Lagaros, V. Plevris, Multi-objective optimization of skeletal structures under static and seismic loading conditions, *Engrg. Opt.* 34 (2002) 645–669.
- [2] D.N. Chu, Y.M. Xie, A. Hira, G.P. Steven, Evolutionary structural optimization for problems with stiffness constraints, *Finite Elements Anal. Des.* 21 (1996) 239–251.
- [3] S. Adali, Pareto optimal design of beams subjected to support motions, *Comput. Struct.* 16 (1983) 297–303.
- [4] M.E. Botkin, Shape optimization with multiple loading conditions and mesh refinement, *AIAA J.* 28 (1990) 922–927.
- [5] A.R. Diaz, M.P. Bendsoe, Shape optimization of structures for multiple loading conditions using a homogenization method, *Struct. Opt.* 4 (1992) 17–22.
- [6] M.P. Bendsoe, A.R. Diaz, R. Lipton, J.E. Taylor, On the prediction of extremal material properties and optimal material distribution for multiple loading conditions, *ASME Adv. Des. Automat. DE-69* (2) (1994) 213–220.
- [7] M.P. Bendsoe, A.R. Diaz, R. Lipton, J.E. Taylor, Optimal design of material properties and material distribution for multiple loading conditions, *Int. J. Numer. Methods Engrg.* 38 (1995) 1149–1170.
- [8] M. Shimoda, H. Azegami, T. Sakurai, Multi-objective shape optimization of linear elastic structures considering multiple loading conditions, *JSME Int. J., Ser. A* 39 (1996) 407–414.
- [9] W. Gutkowsky, K. Dems, Shape optimization of a 2D body subjected to several loading conditions, *Engrg. Opt.* 29 (1997) 293.
- [10] B. Haridas, W.K. Rule, A modified interior penalty algorithm for the optimization of structures subjected to multiple independent load cases, *Comput. Struct.* 65 (1997) 69–81.
- [11] E.J. O'Brien, A.S. Dixon, Optimal plastic design of pitched roof frames for multiple loading, *Comput. Struct.* 64 (1997) 737–740.
- [12] M. Papadrakakis, N.D. Lagaros, Y. Tsompanakis, V. Plevris, Large scale structural optimization: Computational methods and optimization algorithms, *Arch. Computat. Methods Engrg.* 8 (2001) 239–301.
- [13] K.M. Mueller, M. Liu, S.A. Burns, Fully stressed design of frame structures and multiple load paths, *J. Struct. Engrg.—ASCE* 128 (2002) 806–814.
- [14] D. Wang, W.H. Zhang, J.S. Jiang, Truss shape optimization with multiple displacement constraints, *Comput. Methods Appl. Mech. Engrg.* 191 (2002) 3597–3612.
- [15] Y.M. Xie, G.P. Steven, Optimal design of multiple load case structures using an evolutionary procedure, *Engrg. Comput.* 11 (1994) 295–302.
- [16] Y.M. Xie, G.P. Steven, *Evolutionary Structural Optimization*, Springer-Verlag, Berlin, 1997.
- [17] V. Young, O.M. Querin, G.P. Steven, Y.M. Xie, 3D and Multiple Load Case Bidirectional Evolutionary Structural optimization (BESO), *Struct. Opt.* 18 (1999) 183–192.
- [18] Q. Li, G.P. Steven, Y.M. Xie, Evolutionary thickness design with stiffness maximization and stress minimization criteria, *Int. J. Numer. Methods Engrg.* 52 (2001) 979–995.
- [19] Q. Li, G.P. Steven, Y.M. Xie, Thermoelastic topology optimization for problems with varying temperature fields, *J. Thermal Stress.* 24 (2001) 347–366.
- [20] B. Esping, Design optimization as an engineering tool, *Struct. Opt.* 10 (1995) 137–152.
- [21] M. Kocvara, M. Zibulevsky, J. Zowe, Mechanical design problems with unilateral contact, *Math. Model. Numer. Anal.* 32 (1998) 255–282.
- [22] A. Ben-Tal, M. Kocvara, A. Nemirovski, J. Zowe, Free material design via semidefinite programming: the multiloading case with contact conditions, *SIAM Rev.* 42 (2000) 695–715.

- [23] W. Li, G.P. Steven, Y.M. Xie, Shape design for two- and three-dimensional contact problems using an evolutionary method, *Int. J. Comput. Eng. Sci.* 2 (2001) 181–198.
- [24] W. Li, Q. Li, G.P. Steven, Y.M. Xie, An evolutionary shape optimization procedure for contact problem in mechanics designs, *Proc. Inst. Mech. Eng. Part C—J. Mech. Engrg. Sci.* 217C (2003) 435–446.
- [25] Y. Tada, N. Nishihara, Optimum shape design of contact surface with finite element method, *Adv. Engrg. Software* 18 (1993) 75–85.
- [26] J.T. Oden, G.F. Carey, *Finite Elements: Special Problems in Solid Mechanics, Volume V*, Prentice-Hall Inc, New Jersey, 1984.
- [27] Z.H. Zhong, J. Mackerle, Contact-impact problems: a review with bibliography, *ASME Trans. Appl. Mech. Rev.* 47 (1994) 55–76.
- [28] G + D Computing, *Strand6 Finite Element Analysis System Reference Manual and User Guide* (G + D Computing Pty Ltd, 1993).
- [29] N. Zabarar, S. Ganapathysubramanian, Q. Li, A continuum sensitivity method for the design of multi-stage metal forming processes, *Int. J. Mech. Sci.* 45 (2003) 325–358.
- [30] D. Hilding, A. Klarbring, J. Petersson, Optimization of structures in unilateral contact, *ASME Trans., Appl. Mech. Rev.* 52 (1999) 139–160.
- [31] E.A. Fancello, J. Haslinger, R.A. Feijoo, Numerical comparison between two cost functions in contact shape optimization, *Struct. Opt.* 9 (1995) 57–68.
- [32] J. Haslinger, P. Neittaanmaki, *Finite Element Approximation for Optimal Shape, Material and Topology Design*, John Wiley & Sons, Chichester, 1996.
- [33] E.J. Haug, B.M. Kwak, Contact stress minimization by contour design, *Int. J. Numer. Methods Engrg* 12 (1978) 917–930.
- [34] N. Kikuchi and J.E. Taylor, Shape optimization for unilateral elastic contact problems, in: *Numerical Methods in Coupled Problems, Proceedings of International Conference at University College, Swansea, Wales, 1981*, pp. 430–441.
- [35] V. Pareto, *Manuale di Economica Politica*, Societa Editrice Libreria, Milan, (1906); translated into English by A.S. Schwier as *Manual of Political Economy*, edited by A.S. Schwier and A.N. Page, 1971. New York: A.M. Kelley.
- [36] K.A. Proos, G.P. Steven, O.M. Querin, Y.M. Xie, Multicriterion evolutionary structural optimization using the weighting and the global criterion methods, *AIAA J.* 39 (2001) 2006–2012.
- [37] P. Pedersen, L. Jørgensen, Minimum mass design of elastic frames subjected to multiple load cases, *Comput. Struct.* 18 (1984) 147–157.
- [38] R.T. Marler, J.S. Arora, Survey of multi-objective optimization methods for engineering, *Struct. Multidisciplinary Opt.* 26 (2004) 369–395.
- [39] K.I. Tsubota, T. Adachi, Y. Tomita, Functional adaption of cancellous bone in human proximal femur predicted by trabecular surface remodeling simulation toward uniform stress state, *J. Biomech.* 35 (2002) 1541–1551.
- [40] E. Bångtsson, D. Noreland, M. Berggren, Shape optimization of an acoustic horn, *Comput. Methods Appl. Mech. Engrg.* 192 (2003) 1533–1571.
- [41] P. Podra, S. Andersson, Finite element analysis wear simulation of a conical spinning contact considering surface topography, *Wear* 224 (1999) 13–21.
- [42] I. Das, J.E. Dennis, A closer look at drawbacks of minimizing weights sums of objective for Pareto set generation in multicriteria optimization problems, *Struct. Opt.* 14 (1997) 63–69.
- [43] I. Das, J.E. Dennis, Normal-boundary intersection: A new method for generating the Pareto surface in nonlinear multicriteria optimization problems, *SIAM J. Opt.* 8 (1998) 631–657.